

SIMULATING BEAM TRANSPORT WITH PERMANENT MAGNET CHICANE FOR THz FEL

A. Fisher*, Y. Park, M. Lenz, A. Ody, P. Musumeci†, UCLA, Los Angeles, USA
R. Agustsson, T. Hodgetts, A. Murokh, RadiaBeam Technologies, Santa Monica, USA

Abstract

Free electron lasers are an attractive option for high average and peak power radiation in the THz gap, a region of the electromagnetic spectrum where radiation sources are scarce, as the required beam and undulator parameters are readily achievable with current technology. However, slippage effects require the FEL to be driven with relatively long and low current electron bunches, limiting amplification gain and output power. Previous work demonstrated that a waveguide could be used to match the radiation and e-beam velocities in a meter-long strongly-tapered helical undulator, resulting in 10% energy extraction from an ultrashort 200 pC, 5.5 MeV electron beam. We present simulations for a follow-up experiment targeting higher frequencies with improvements to the e-beam transport including a permanent magnet chicane for strong beam compression. FEL simulations show >20% extraction efficiency from a 125 pC, 7.4 MeV electron beam at 0.32 THz.

INTRODUCTION

Compact and efficient high average and peak power radiation sources are in high demand for scientific and industrial applications including time-domain spectroscopy, high field resonant and non-resonant excitation of solid state systems, and THz-based imaging for medical and security [1, 2]. Free Electron Lasers (FELs) use the ponderomotive interaction between an electromagnetic wave and a relativistic electron beam copropagating in a magnetic undulator and are an attractive source in the 0.1-10 THz range as the necessary undulator and beam parameters are easily achievable [3, 4]. Addition advantages include high peak power and repetition rates limited only by the electron beam provided. FEL facilities have already played an important role in the development of THz science [5–10], with more facilities coming online [11–13] and being planned for the future [14–16].

Our previous experiment [17] showed that by using a waveguide to contain diffraction and match group velocities, a 10% extraction efficiency could be achieved from an ultrashort 200 pC, 5.5 MeV beam. After reviewing the zero-slippage conditions in a waveguide FEL, we investigate a proposed follow-up experiment to double the frequency of THz produced. We discuss improvements to the beamline, a design for a tunable permanent magnet chicane, and the consequences of increasing the resonant frequency. Start to end simulations are presented for the electron beam transport and FEL interaction.

* afisher000@g.ucla.edu

† musumeci@physics.ucla.edu

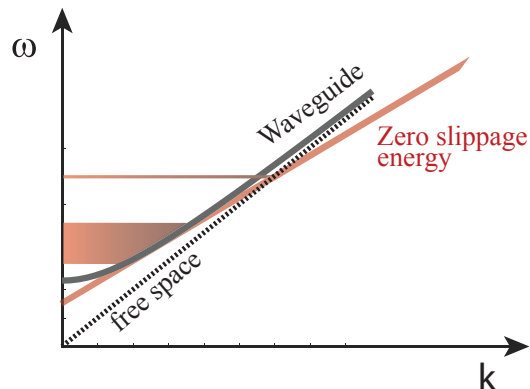


Figure 1: Dispersion diagram for a waveguide FEL. Electrons (red) in free space can only be resonant at a single frequency, whereas a waveguide allows interaction over a large bandwidth.

ZERO-SLIPPAGE RESONANCE

The zero-slippage FEL interaction requires satisfying the traditional FEL phase resonance condition, $(k_z + k_u) = \frac{\omega}{\beta_z c}$ and the group-velocity or zero-slippage condition, $\frac{c^2 k_z}{\omega} = \beta_z c$. In these expressions, the longitudinal wavevector k_z and radiation frequency ω are connected by the waveguide dispersion relation $\omega^2/c^2 = k_z^2 + k_\perp^2$ where $k_\perp = 1.8412/R$ for the TE11 circular waveguide mode [18], R is the waveguide radius, $k_u = 2\pi/\lambda_u$ where λ_u is the undulator period, and $c\beta_z$ is the longitudinal beam velocity in the undulator. Figure 1 illustrates the large bandwidth interaction when the phase velocity (point) and group velocity (slope) are adequately matched.

It can be shown from these conditions that the resonant frequency at zero-slippage is given by $2\pi f_{zs} = ck_u \beta_{z0} \gamma_{z0}^2$ where $\gamma_{z0} = \gamma_0/\sqrt{1+K^2}$. For relativistic beams, $\gamma_0 = \frac{k_\perp}{k_u} \sqrt{1+K^2}$ and we see that for given waveguide and undulator parameters, the resonant beam energy is uniquely determined.

To maintain resonance with the decelerating electrons, the magnetic field strength must be strongly tapered along the undulator to enhance the stimulated superradiant radiation emission (TESSA) of the electrons [19].

A final consequence of the zero-slippage conditions is that the ratio of the helical beam trajectory radius to the waveguide radius is $\frac{r_{max}}{R} = \frac{1}{1.8412} \frac{K}{\sqrt{1+K^2}} \leq 0.543$ with an upper bound independent of frequency.

BEAM TRANSPORT

It is important to demonstrate the scalability of the waveguide FEL interaction to higher frequencies in the THz gap for broader scientific application. In Table 1 we list the simulated parameters for an experiment doubling the target frequency to 320 GHz. Electron beam parameters are quoted at the undulator entrance.

Table 1: Simulation Parameters

Electron Beam		Chicane	
γ	14.5	Gap	8 mm
σ_γ/γ	0.7%	B_y	270 mT
σ_x, σ_y	139 μm , 122 μm	θ_{bend}	30deg
σ_z	90 μm	R_{56}	0.05 m
$\epsilon_{n,x}, \epsilon_{n,y}$	5 mm·mrad		
Undulator		Waveguide	
$K_{rms,0}$	2.18	Material	Cu
λ_u	3.2 cm	Radius	1.6 mm
N_u	30		

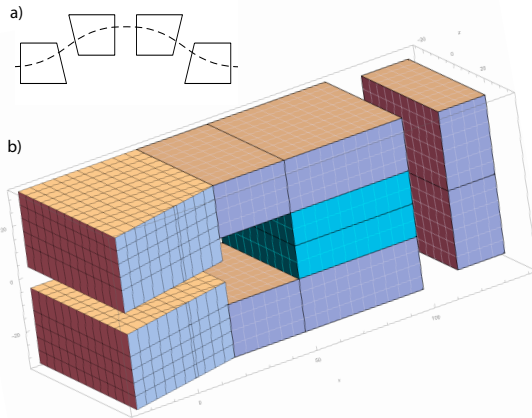


Figure 2: RADIA model of chicane.

We note that targeting higher frequencies relaxes a couple experimental constraints. First, the diffraction of the produced radiation is diminished, allowing easier transport to and within the THz diagnostics. We have also redesigned and shortened the vacuum system immediately after the undulator to remove apertures that could clip the THz beam. Secondly, the radius of the electron trajectory is reduced, increasing the tuning precision for hall probe and pulsed wire measurements which are practically limited to the magnetic axis by the enclosed helical geometry.

The challenges of an experiment producing higher frequency THz include focusing to a smaller matched spot-size determined by undulator focusing and compressing to achieve bunching factors that can seed the FEL interaction.

A quadrupole triplet was previously used to focus the e-beam into the undulator, but the large distance (1.2 m)

required by beamline real estate constraints limited the minimum spotsize. The mismatched e-beam experienced betatron oscillations in the undulator, reducing charge transmission and degrading the interaction. We have since added a solenoid 30 cm before the undulator to supply the necessary focusing strength to match the 7.4 MeV e-beam into the undulator while the quadrupole triplet is used to symmetrize the beam at the solenoid.

At longer wavelengths, compression of the ebeam could be achieved by tuning the amplitude and phase of a booster linac to both accelerate the beam to the resonant energy and provide an energy chirp to compress the e-beam in the drift to the undulator. Limitations on the maximum accelerating gradient and drift length remove this option for achieving a significant bunching factor at shorter wavelengths. Lengthening the beam by stretching the laser pulse illuminating the cathode reduces space charge effects and strengthens the chirp from the linac, but is still insufficient and would result in large energy spread.

We have instead designed a tuneable permanent magnet chicane using the modeling software RADIA [20] that can achieve compression with a reduced energy chirp, minimizing the e-beams energy spread in the FEL interaction. Figure 2 shows the RADIA model for a single chicane magnet where field lines from the 5 cm x 5 cm blue permanent magnets are guided across the trapezoidal-shaped 8 mm gap via iron yokes. The small bending radius (10 cm) results in a large deflection (30 deg) of the ebeam and significant transverse focusing effects. We chose to split the focusing equally between the x and y directions using a 15 deg shapping of the poles between magnets 1,2 and 3,4. Each chicane magnet has an iron shim that can be adjusted to divert field lines, reducing the peak field by 20% in order to align the electron beam or adjust the R56.

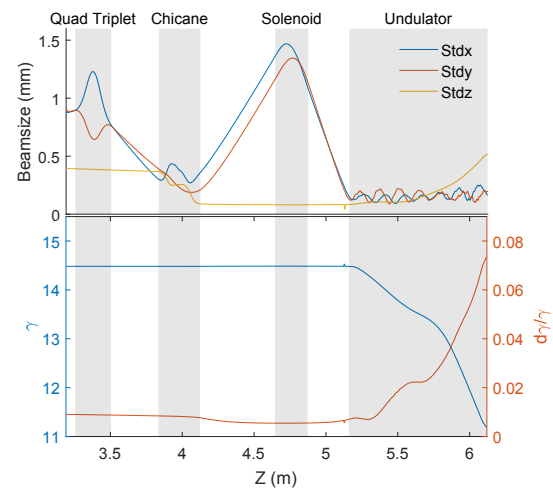


Figure 3: Electron beam transport.

The linac induced energy chirp and chicane field strengths can be tuned to compress beams with relativistic factors in the range $\gamma = 14 - 16$, enabling us to study the energy resonance of the zero-slippage regime.

Figure 3 shows the beamline transport done with the General Particle Tracer code [21] for a 2 ps FWHM laser pulse. After exiting the chicane, the strongly divergent e-beam is focused with the solenoid into the undulator. Although space charge effects will be increased when the beam is both focused and compressed at the exit of the chicane, simulations show a bunching factor of >0.8 is still achieved with only a 40% growth in the transverse emittance.

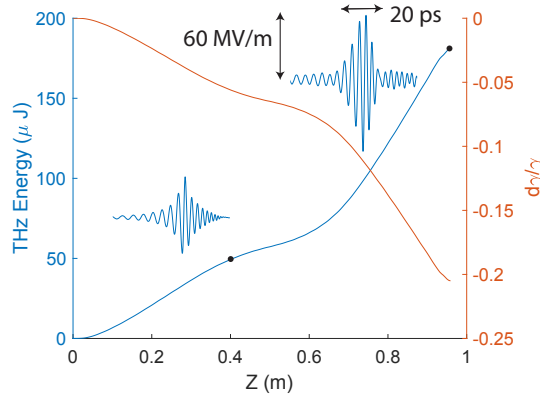


Figure 4: FEL interaction along undulator.

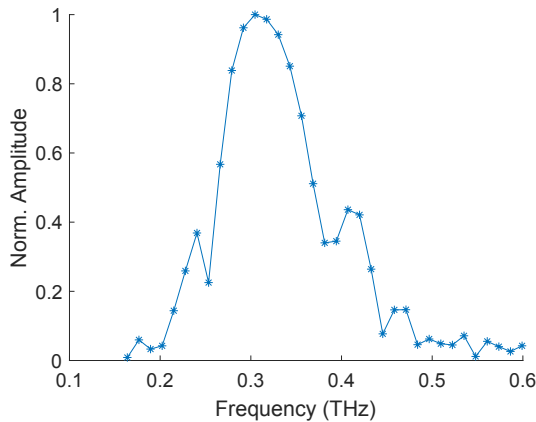


Figure 5: THz spectrum.

FEL INTERACTION

The FEL interaction is simulated with a GPT extension module [22] that self-consistently calculates the interaction of electrons and electromagnetic fields inside the undulator taking into account both dispersion and 3D space charge effects.

Results are shown for a 125 pC bunch with the same undulator tapering as in the previous experiment for comparison. At higher frequencies, the smaller waveguide area implies that a smaller amount of charge is necessary to excite large electric field amplitudes and achieve significant conversion efficiencies. A design tradeoff exists between a desire to maximize charge in the FEL and a need to reduce space charge effects in the beam transport.

To physically achieve a smaller waveguide radius, we place a tight fitting copper pipe inside the vacuum waveguide. This is an improvement from before when the stainless steel vacuum pipe doubled as the waveguide, introducing noticeable power loss in the waveguide. At the same time, the copper waveguide will be supported by the vacuum pipe, simplifying the alignment.

Figure 4 shows the FEL interaction along the undulator with an impressive 20% average deceleration of the electron beam producing a 20 ps, 175 μJ THz pulse. These results emphasize the importance of strong bunching and full charge transmission in the FEL interaction. Figure 5 shows the large bandwidth of the zero-slippage resonance, with frequency components extending beyond 0.4 THz.

CONCLUSION

Simulations show promising results for operating the zero-slippage waveguide FEL at higher frequencies with 20% energy extraction from a 125 pC, 7.4 MeV beam. This highlights the importance of our beamline improvements including a solenoid for transverse focusing and a permanent magnet chicane to achieve significant bunching factors at shorter wavelengths. Demonstrating full transmission through the undulator at the resonant energy would imply more aggressive tapering could be achieved with a large bunch charge. Future work could include recirculating a fraction of the produced radiation to seed successive passes in the undulator [23].

ACKNOWLEDGEMENTS

This work was supported by NSF grant PHY-1734215 and DOE grant No. DE-SC0009914 and DE-SC0021190. The undulator construction has been carried out under SBIR/STTR DE-SC0017102 and DE-SC0018559.

REFERENCES

- [1] S. Dhillon *et al.*, “The 2017 terahertz science and technology roadmap,” *Journal of Physics D: Applied Physics*, vol. 50, no. 4, p. 043001, 2017.
- [2] Y.-S. Lee, *Principles of terahertz science and technology*. Springer Science & Business Media, 2009, vol. 170.
- [3] A.-S. Müller and M. Schwarz, “Accelerator-based thz radiation sources,” *Synchrotron Light Sources and Free-Electron Lasers: Accelerator Physics, Instrumentation and Science Applications*, pp. 83–117, 2020.
- [4] G. P. Gallerano and S. G. Biedron, “Overview of Terahertz Radiation Sources,” in *Proc. FEL’04*, Trieste, Italy, Aug.-Sep. 2004, pp. 216–221.
- [5] L. Elias, “Free-electron laser research at the university of california, santa barbara,” *IEEE journal of quantum electronics*, vol. 23, no. 9, pp. 1470–1475, 1987.
- [6] G. Ramian, “The new ucsb free-electron lasers,” *Nuclear Instruments and Methods in Physics Research Section A: Accelerators, Spectrometers, Detectors and Associated Equipment*, vol. 318, no. 1-3, pp. 225–229, 1992.
- [7] D. Oepts, A. Van der Meer, and P. Van Amersfoort, “The free-electron-laser user facility felix,” *Infrared physics & technology*, vol. 36, no. 1, pp. 297–308, 1995.

- [8] G. Gallerano, A. Doria, E. Giovenale, and A. Renieri, "Compact free electron lasers: From cerenkov to waveguide free electron lasers," *Infrared physics & technology*, vol. 40, no. 3, pp. 161–174, 1999.
- [9] Y. U. Jeong *et al.*, "First lasing of the kaeri compact far-infrared free-electron laser driven by a magnetron-based microtron," *Nuclear Instruments and Methods in Physics Research Section A: Accelerators, Spectrometers, Detectors and Associated Equipment*, vol. 475, no. 1-3, pp. 47–50, 2001.
- [10] B. Knyazev, G. Kulipanov, and N. Vinokurov, "Novosibirsk terahertz free electron laser: Instrumentation development and experimental achievements," *Measurement Science and Technology*, vol. 21, no. 5, p. 054017, 2010.
- [11] M. Gensch *et al.*, "THz Facility at ELBE: A Versatile Test Facility for Electron Bunch Diagnostics on Quasi-CW Electron Beams," pp. 933–934, doi:10.18429/JACoW-IPAC2014-TUZA02
- [12] X. Shu, Y. Dou, X. Yang, M. Li, H. Wang, and X. Lu, "First lasing of caep thz fel facility," in *2017 42nd International Conference on Infrared, Millimeter, and Terahertz Waves (IRMMW-THz)*, IEEE, 2017, pp. 1–2.
- [13] H.-T. Li, Q.-K. Jia, S.-C. Zhang, L. Wang, and Y.-L. Yang, "Design of felichem, the first infrared free-electron laser user facility in china," *Chinese Physics C*, vol. 41, no. 1, p. 018102, 2017.
- [14] R. S. Romaniuk, "Polfel-free electron laser in poland," *Photonics Letters of Poland*, vol. 1, no. 3, pp. 103–105, 2009.
- [15] A. Nause *et al.*, "6 mev novel hybrid (standing wave-traveling wave) photo-cathode electron gun for a thz superradiant fel," *Nuclear Instruments and Methods in Physics Research Section A: Accelerators, Spectrometers, Detectors and Associated Equipment*, p. 165547, 2021.
- [16] P. Boonpornprasert *et al.*, "Start-to-End Simulations for IR/THz Undulator Radiation at PITZ," in *Proc. FEL'14*, Basel, Switzerland, Aug. 2014, pp. 153–158, <https://jacow.org/FEL2014/papers/MOP055.pdf>
- [17] A. Fisher *et al.*, "Single-pass high-efficiency terahertz free-electron laser," *Nature Photonics*, pp. 1–7, 2022, doi:10.1038/s41566-022-00995-z
- [18] A. Zangwill, *Modern electrodynamics*. Cambridge University Press, 2013.
- [19] J. Duris, A. Murokh, and P. Musumeci, "Tapering enhanced stimulated superradiant amplification," *New Journal of Physics*, vol. 17, no. 6, p. 063036, 2015.
- [20] O. Chubar, P. Elleaume, and J. Chavanne, "A three-dimensional magnetostatics computer code for insertion devices," *Journal of synchrotron radiation*, vol. 5, no. 3, pp. 481–484, 1998.
- [21] M. J. de Loos and S. B. van der Geer, "General Particle Tracer: A New 3D Code for Accelerator and Beamline Design," in *Proc. EPAC'96*, Sitges, Spain, Jun. 1996, pp. 1245–1247.
- [22] A. Fisher, P. Musumeci, and S. Van der Geer, "Self-consistent numerical approach to track particles in free electron laser interaction with electromagnetic field modes," *Physical Review Accelerators and Beams*, vol. 23, no. 11, p. 110702, 2020.
- [23] J. Duris, P. Musumeci, N. Sudar, A. Murokh, and A. Gover, "Tapering enhanced stimulated superradiant oscillator," *Phys. Rev. Accel. Beams*, vol. 21, p. 080705, 8 2018, doi:10.1103/PhysRevAccelBeams.21.080705